

# Flow Analysis with Cerium (IV) Colorimetric Reagent for Determination of Procaine and Elucidation of the Color Species by Computational Investigation

Yuthana Tantirungrotechai, Aphiradee Syananondh, Napaporn Youngvises\*

*Division of Chemistry, Faculty of Science and Technology, Thammasat University,  
Pathum Thani 12120, Thailand*

Received 16 June 2021; Received in revised form 25 August 2022

Accepted 13 September 2022; Available online 20 March 2023

## ABSTRACT

Flow injection analysis (FIA) with spectrometric detection was applied to determine procaine hydrochloride (PR) based on the reaction of procaine and cerium (IV) sulfate tetrahydrate produced a red compound that be enhanced sensitivity by adding sodium dodecyl sulfate (SDS). A calibration graph was linear in the range of 1-150 mg L<sup>-1</sup> of PR with R<sup>2</sup> of 0.9998. The detection limit (3S/N) was 0.75 mg L<sup>-1</sup>. Percentage recoveries and relative standard deviation were 100-108 and 2.9, respectively. To help elucidating the colored species, the density functional theory and the time-dependent density functional theory were used to calculate the relative energies and the absorption spectra of all possible complexes involved in the reaction. The calculation suggests that a Ce(IV) could initially form a complex with procaine at the carbonyl oxygen and cause ester hydrolysis leading to a more stable Ce(IV)/PABA complex in solution. The proposed method was applied to determine PR in pharmaceutical and cosmetic preparation and compared to USP 2004. At 95% confidence, there was no significant difference between the results of both methods. The method should provide an accessible and eco-friendly way to determine PR in a typical laboratory.

**Keywords:** Cerium (IV); Colorimetry; Density functional theory; Flow injection analysis; Procaine

## 1. Introduction

Procaine hydrochloride (PR) or 2-diethylaminoethyl 4-aminobenzoate hydrochloride is a local anesthetic of the ester type that has a slow onset and a short duration of action. It is mainly used for infiltration anesthesia, peripheral nerve block, and spinal block [1]. Not only known for its pharmaceutical preparation, procaine has also been commercialized as anti-aging treatments in Romania.

Several quantitative methods, such as high performance liquid chromatographic [2, 3], capillary electrophoresis [4], electrochemical [5] and spectroscopic techniques [6-14] have been introduced to determine the amount of procaine in pharmaceuticals. Chromatographic and capillary electrophoresis techniques require sophisticated and expensive instruments. Although chromatography is the most popular technique in separation and determination, the time consuming, sophisticated procedure, high operating cost and waste generation are considered as disadvantages for this technique. On the other hand, the electro-chemical method using a modified electrode can provide a rapid response. However, this method still requires expertise to achieve the reproducible response. Various spectroscopic techniques, e.g. chemiluminescence [15], fluorescence [16] and UV-visible spectrometry [7] have been used in PR determination. The standard official method, USP 2004 [17], is based on the extraction of PR in chloroform and the absorbance measurement at 280 nm. Nevertheless, not only is a large amount of extracted solvent used, but a large amount of waste is also generated. Moreover, the routine analysis based on this method can be very time- and labor-intensive.

In this work we suggest another simple and efficient analysis method to determine the amount of PR based on colorimetry. We prefer the colorimetric method as it is readily available method at most laboratories due to a simple instrument

involved, its relative simplicity and low cost. Both organic compounds and metal ions have been proposed as colorimetric reagents in the literature, for example; 4-dimethyl-aminocinnamaldehyde [12] (with stopped-flow method), p-dimethylamino-benzaldehyde [9], p-benzoquinone [10], 1,2-naphthoquinone-4-sulfonic acid [11], phenol [18] and iron(III) [8]. The usage of iron(III) is based on the conversion of PR into 4-amino-benzohydroxyamic acid (PABA) which reacts with iron(III) forming a violet complex. Most of these reagents provide a narrow range of linearity except in the case of 1,2-naphthoquinone-4-sulfonic acid with sodium lauryl sulfate as a sensitizing agent [11].

We propose the use of cerium (IV) sulfate tetrahydrate as a new colorimetric reagent for the determination of PR incorporating with FIA technique. The effect of some surfactants to enhance the sensitivity of this analytical reaction was studied. To understand the studied reaction at a molecular level, we employed the density functional theory (DFT) and the time-dependent density functional theory (TDDFT) to calculate the relative energies and the absorption spectra of all possible complexes involved in the reaction. The computational investigation should give us some insights into the colored species in the observed solution.

## 2. Materials and Methods

### 2.1 Instrumentation

A peristaltic pump and six-port valve (from FIA Lab, USA) with spectrometer (Jenway 6051, UK) was used in this work with a simple two-line FIA manifold (Fig. 1) consisting of 0.8 mm i.d. polyethylene tubing and T-way (Elkay, Hampshire, England). The signal was recorded by eDAQ software, Australia. A Shimadzu UV-1700 UV-Visible spectrometer (Japan) was used to scan spectrum and study the reaction time during the preliminary study.

## 2.2 Reagents

All chemicals used in this experiment were analytical grade. Procaine hydrochloride (PR) and sodium dodecyl sulfate (SDS) were purchased from Sigma (St. Louis, USA). Cerium sulfate tetrahydrate (Ce (IV)) and sulfuric acid ( $\text{H}_2\text{SO}_4$ ) were purchased from BDH. Distilled water was used throughout the experiment.

The colorimetric reagent (as a reagent stream in FIA) was freshly prepared as follows: 0.2021 g of cerium sulfate tetrahydrate (Ce(IV)) was weighed and transferred to a 250.0 mL volumetric flask, dissolved by 150 mL of 0.2 mol  $\text{L}^{-1}$  of  $\text{H}_2\text{SO}_4$ ; then 0.1442 g of SDS was added to this solution. After SDS was completely dissolved, the solution was diluted to volume using  $\text{H}_2\text{SO}_4$ .

## 2.3 Standard preparation

Stock standard solution 1,000 mg  $\text{L}^{-1}$  of PR was prepared by dissolving 0.1000 g in distilled water until the final volume was 100.0 mL. Other concentrations can be prepared by diluting the standard solution with distilled water.

## 2.4 Sample preparation

Five commercials of some injectable ampoules from Europe and USA (Injection samples A-E) were local anesthetic pharmaceuticals and anti-aging products. Sample solution was prepared by mixing 20 vials of 1-2 % w/v of procaine hydrochloride injections. A 1.0 mL of this mixed sample was pipetted and transferred to a 100.0 mL volumetric flask and, then diluted further with distilled water until the concentration was about 10 mg  $\text{L}^{-1}$ .

Five commercial procaine hydrochloride tablets from Romania and USA were samples of anti-aging products denoted as Tablet samples A-E. Twenty tablets were weighed, ground and mixed. The powder was accurately weighed equivalent to 100 mg of PR, transferred to a

100 mL-volumetric flask, 50 mL of water was added, the solution was sonicated for 5 mins and diluted to volume with distilled water. After filtration, 10 mg  $\text{L}^{-1}$  of sample solution was further prepared in a 25-mL volumetric flask.

## 2.5 FIA procedure

A two-line FIA manifold was investigated (Fig. 1). It consisted of water as a carrier stream and a mixture of Ce (IV) and SDS in  $\text{H}_2\text{SO}_4$  as a reagent stream. Three replicate injections were employed throughout the experiment. The peak height was measured in mV by eDAQ software.

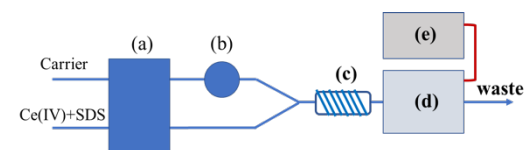


**Fig. 1.** Schematic diagram of two-line FIA manifold using water as carrier and Ce(IV) + SDS in  $\text{H}_2\text{SO}_4$  as reagent stream; (a) peristaltic pump; (b) six-port valve; (c) reaction coil; (d) spectrometer and (e) computer.

The starting condition was 0.2 mmol  $\text{L}^{-1}$  of Ce(IV) mixed with 0.01 mol  $\text{L}^{-1}$  SDS in 0.2 mol  $\text{L}^{-1}$   $\text{H}_2\text{SO}_4$  as a reagent stream and water as a carrier stream. The physical manifold consisted of 80 cm coil length, 190  $\mu\text{L}$  sample loop and 1.6 mL  $\text{min}^{-1}$  flow rate. The detection wavelength was set at 513 nm. Each variable was investigated by univariate optimization. The PR at concentrations of 5, 10, 20 and 40 mg  $\text{L}^{-1}$  was injected into the FIA system. The calibration curve was then constructed by linear regression method. To select the best condition, the sensitivity (mV  $\text{L mg}^{-1}$ ) was considered. The optimal conditions in terms of chemicals and physical manifold parameters were studied.

## 2.6 Computational Investigations

We considered all possible configurations of procaine and its products after reacting with Ce(IV). Procaine can be

hydrolysed at the ester bond which yields 4-aminobenzohydroxyamic acid (PABA) and diethylaminoethanol (DEAE) as products. Since procaine, PABA and DEAE ligands have several donor atoms (see Fig. 2.), there may be several possible binding configurations between Ce(IV) and these organic ligands. We tried to find all possible binding configurations of Ce(IV) complexes and locate the most stable configuration. All possible binding configurations were initially constructed by placing Ce(IV) at locations close to each donor atom of the ligand. The possibilities of monodentate and bidentate configurations were considered. We limited our treatment to a 1:1 ratio of metal:ligand as guided by the preliminary result of Job's method. To avoid a large positive charge in the calculation and to neutralize the overall structure, four fluoride ligands were bound to metal cerium [19-22]. This {Ce(IV)F<sub>4</sub>} metal fragment was used to bind with procaine or its hydrolyzed products, DEAE and PABA. An additional water molecule was added to some Ce(IV) complexes in this study to obtain an octahedral arrangement. Geometry optimization was conducted from these initial structures in the gaseous state. The lowest energy structure was identified as the most stable configuration among all optimized structures [23]. To compare complexes formed from different ligands, we arbitrarily chose one binding configuration as a reference. The stability of

each configuration was measured relative to this reference state while taking the stoichiometric balance into account. The B3LYP and BP86 functionals with the SDD basis set were used in our calculations [24, 25]. The charge density fitting algorithm was used in the case of the BP86 functional to speed up the calculation. The relativistic correction was included in the Stuttgart-Dresden effective core potential of cerium which belongs to the lanthanide series.

Finally, we investigated the optical properties of the Ce(IV)/procaine, Ce(IV)/PABA and Ce(IV)/DEAE systems within the time-dependent density functional theory framework (TDDFT). The TD-PBE0/SDD with the CPCM solvation model [26] was used to calculate the electronic transitions of the most stable configuration for all considered complexes which can be of charge-transfer character [27-30]. We compared the calculated electronic transitions of Ce(IV) complexes with the experimental absorption spectrum of Ce(IV):procaine mixture. To prepare the Ce(IV):procaine mixture, an excess amount of procaine was used to mask the yellow color originating from free Ce(IV) species. The absorption spectrum was recorded using a Shimadzu UV-1700 UV-Visible spectrometer.

All calculations were conducted by using Gaussian 09 [31]. Graphical visualizations were carried out by using Avogadro [32] and XYZviewer [33].

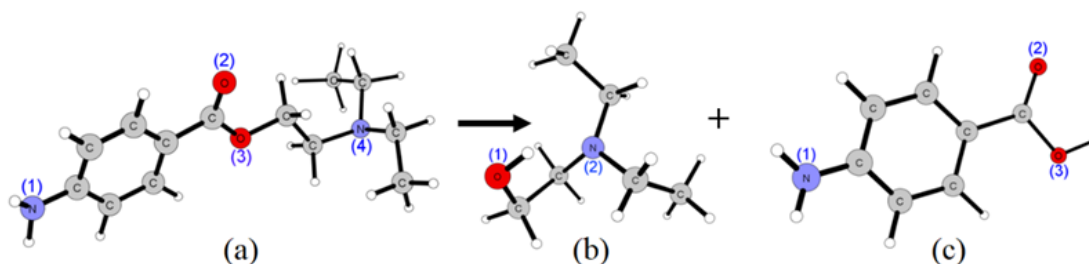


**Fig. 2.** Procaine (a) and its hydrolyzed products, DEAE (b) and PABA (c). The electron donor atoms are labeled in this figure.

### 3. Results and Discussion

#### 3.1 UV-Visible spectrophotometry study of PR and Ce(IV) reaction

The spectra of PR and Ce(IV) in  $\text{H}_2\text{SO}_4$  were presented in Fig. 3(a), in the range of 200-800 nm. The PR solution is colorless while the solution of Ce(IV) in  $\text{H}_2\text{SO}_4$  is yellow. The reaction of PR (2 mmol  $\text{L}^{-1}$ ) and Ce (IV) (1 mmol  $\text{L}^{-1}$ ) in  $\text{H}_2\text{SO}_4$  (0.2 mol  $\text{L}^{-1}$ ) produced red color and spectrum was also shown as line C in Fig.3(a). The product of this reaction presented the wavelength of maximum absorbance ( $\lambda_{\text{max}}$ ) of 495 nm. The red product was however unstable and became brown color within a few minutes. Our work confirms what was previously observed by Wang et al.[34] that the red product of Ce(IV) and PR is unstable. It might be that the product was oxidized by the excess Ce(IV). Therefore, it is necessary to scan the spectrum of this solution immediately after mixing PR and Ce (IV).

The red solution observed after mixing PR and Ce(IV) is similar to what Novaković [14] observed as violet solution when using iron(III) as a colorimetric agent. Instead of acting as an oxidizing agent, Ce(IV) can also form a complex with some ligands [14, 35, 36]. Therefore, it is possible that Ce(IV) may form a complex by using electron pairs at carbonyl or amine group. The mole ratio of Ce(IV) and PR in the complex was analyzed by Job's method using various concentrations of Ce(IV) (0 – 1.0 mmol  $\text{L}^{-1}$ ) and PR(1.0 - 0, mmol  $\text{L}^{-1}$ ) while keeping the total concentration constant at 1.0 mmol  $\text{L}^{-1}$ . Each pair of solutions was propelled using a two-line peristaltic pump with the same flow rate (2 mL  $\text{min}^{-1}$ ), and then mixed in the flow-through cell. The absorbances of products were measured at 495 nm by a UV-Visible spectrophotometer. The Job's plot (see Fig. 4) revealed that the mole ratio of Ce(IV) and PR was 1:1. Computational investigations on the complex contributed to the red solution will be discussed later.

#### 3.2 Effect of surfactants

A surfactant is widely used as a sensitizing reagent in spectrophotometry [11, 37]. Xu et al. [11] employed sodium lauryl sulfate to enhance the absorbance of the product of PR and 1,2-naphthoquinone-4-sulfonic acid. Ahmed et al. [37] used cetylpyridinium bromide to sensitize analytical reaction of Ce (IV) with triphenylformazan derivatives.

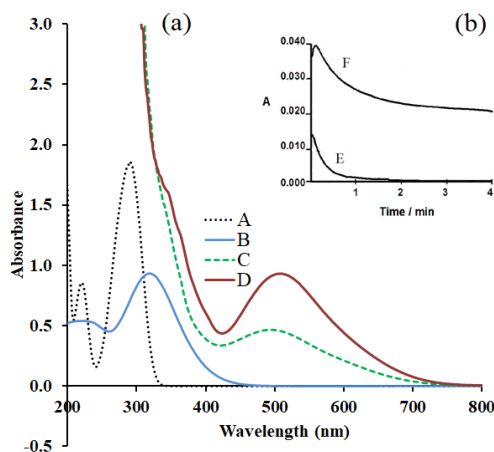


**Fig. 3.** (a) Absorption spectra of 0.1 mmol  $\text{L}^{-1}$  PR in water (line A), 0.2 mmol  $\text{L}^{-1}$ , Ce(IV) in 0.2 mol  $\text{L}^{-1}$   $\text{H}_2\text{SO}_4$  (line B), product of Ce(IV) and PR (line C) and Ce(IV)-PR product with 0.025 mol  $\text{L}^{-1}$  SDS (line D). The concentration of PR and Ce(IV) in the solution for color specie formation were 2 and 1 mmol  $\text{L}^{-1}$ , respectively. All spectra were scanned against blank 0.2 mol  $\text{L}^{-1}$   $\text{H}_2\text{SO}_4$ , excluding PR spectrum against blank water. (b) The study of reaction time and stability of PR and Ce(IV) formation in the system with/without SDS 25 mmol  $\text{L}^{-1}$  (line F and E, respectively), using PR 0.05 mmol  $\text{L}^{-1}$ , Ce(IV) 2 mmol  $\text{L}^{-1}$  in 0.2 mol  $\text{L}^{-1}$   $\text{H}_2\text{SO}_4$ .

In this study, the effects of sodium dodecyl sulfate (SDS), cetyl trimethylammonium bromide (CTAB) and Tween 60 on the absorbance enhancement were tested by adding each surfactant into the reaction of PR and Ce(IV). The results were compared to the absorbance of solution mixture without surfactant.

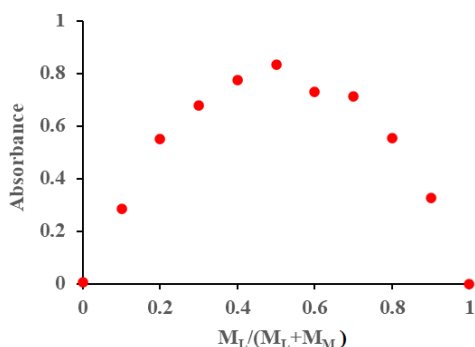


**Fig. 4.** Job's plot for PR:Ce(IV) mole ratio determination using flow system at 495 nm for monitoring absorbance.

Unfortunately, for the case of CTAB, the colloid was formed in the reaction mixture. In the presence of Tween 60, light absorption of product decreased whereas SDS significantly increased the solution absorbance and shifted the  $\lambda_{\max}$  to 513 nm. The SDS-enhanced absorption spectrum is shown as line D in Fig. 3(a). Moreover, the absorbance of reaction mixture prepared from 0.05 mmol L<sup>-1</sup> of PR and 2 mmol L<sup>-1</sup> of Ce(IV), was measured as a function of time (Fig. 3(b)). The results showed that reactions were rapid with or without SDS. Without SDS (line E), the absorption dropped to nearly zero in a few minutes. However, with SDS (line F), the absorption decreased to a non-zero value which suggested that SDS not only increased the sensitivity but also stabilized the product. This suggests that it increased solubility of the complex by interaction with the nonpolar part of ligand (PABA) which is why the  $\lambda_{\max}$  was red shift to 513 nm. This finding agrees with that of Gürcan et al. [38], in which surfactant was used to enhance sensitivity of complex products. Therefore, SDS was chosen to add into the reaction mixture. Due to its rapid reaction and unstable product, FIA was considered to incorporate with colorimeter to determine PR quantity based on this above-mentioned reaction.

### 3.3 FIA optimization

#### 3.3.1 Effect of reagents in FIA system

Various concentrations of Ce(IV) in the range of 0.2–3.0 mmol L<sup>-1</sup> were studied at instantaneous concentration of another reagents. The sensitivity increased with the increasing Ce(IV) concentration from 0.2 to 2.0 mmol L<sup>-1</sup> and became constant beyond this range. Therefore, 2 mmol L<sup>-1</sup> of Ce(IV) was selected for further study. Due to the low solubility of cerium(IV) sulfate tetrahydrate in water, H<sub>2</sub>SO<sub>4</sub> was often used as a solvent of this reagent. The H<sub>2</sub>SO<sub>4</sub> concentrations of 0.02, 0.1, 0.2, 0.3, 0.5, 0.75, 1, 1.5 and 2.0 mol L<sup>-1</sup> were studied. The pH range of the system was 0–1.8. As the pK<sub>a</sub> of PR is 9.3, the PR in this solution would exist only in the protonated form. Fig. 5 presents the effect of H<sub>2</sub>SO<sub>4</sub> concentration on the sensitivity. H<sub>2</sub>SO<sub>4</sub> was used to increase solubility of Ce(IV). The highest sensitivity was achieved at 0.2 mol L<sup>-1</sup> of H<sub>2</sub>SO<sub>4</sub>. Beyond the concentration of 0.2 mol L<sup>-1</sup>, the sensitivity decreased. H<sub>2</sub>SO<sub>4</sub> may act as a catalyst in the oxidation of complex by excess Ce(IV).

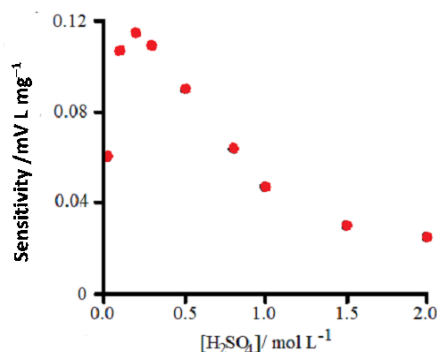


**Fig. 5.** Effect of H<sub>2</sub>SO<sub>4</sub> concentration on the sensitivity.

Because the preliminary study revealed that the SDS concentration affected the absorbance of the product, the optimal SDS concentration was studied next. Fig. 6 shows the optimization of the SDS concentration suitable for the FIA system using the concentrations of 0, 0.2, 0.5, 1, 1.5, 2, 3, 5, 10, 15 and 20 mmol L<sup>-1</sup>. Upon



increasing SDS concentration from 0 to 2.0 mmol L<sup>-1</sup>, the sensitivity increased significantly. Beyond this concentration range, however, the SDS formed micelles and the sensitivity decreased slightly. This indicates that micellar SDS affects the sensitivity to a lesser degree than its monomer form. This suggests that higher concentration of SDS over critical micellar concentration (CMC) presented higher absorbance due to its higher viscosity, then its baseline was higher. The highest sensitivity at 2.0 mmol L<sup>-1</sup> SDS was therefore selected.

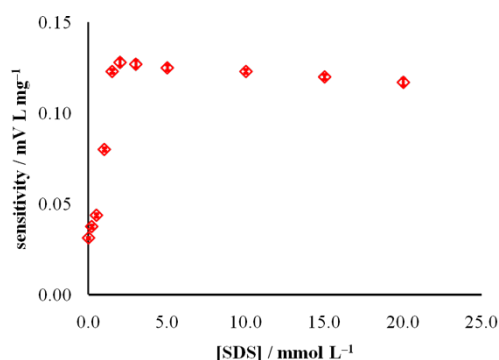


**Fig. 6.** Effect of SDS on the sensitivity of the FIA system.

### 3.3.2 Physical manifold

Due to the fast reaction and unstable product, the effects of physical manifolds such as the length of reaction coil, sample loop and flow rate, on the sensitivity were studied. The sensitivities of the system with the reaction coil length of 0, 30, 50, 65 and 80 cm were 0.08, 0.11, 0.12, 0.11 and 0.10 mV L mg<sup>-1</sup>, respectively. The chosen coil length was 50 cm. Then, the sample loop at 28, 50, 96, 200 and 370 µL was considered leading to the corresponding sensitivities of 0.07, 0.11, 0.17, 0.32 and 0.38 mV L mg<sup>-1</sup>, respectively. We observed that the sensitivity increased with the sample volume. However, to achieve the highest sensitivity possible, the largest amount of sample (370 µL) was required but that caused analysis time to be too long to handle. Therefore, 200 µL sample volume

was selected as an optimal choice for further study. Finally, sensitivities of 0.26, 0.30, 0.39, 0.35 and 0.35 mV L mg<sup>-1</sup> were obtained from the flow rate of 0.6, 1.2, 1.6, 2.2, and 2.8 mL min<sup>-1</sup>, respectively.

Therefore, the optimal condition consisted of 50 cm of reaction coil, 200 µL sample volume and 1.6 mL min<sup>-1</sup> flow rate for this FIA system and the optimal concentration of cerium (IV) sulfate tetrahydrate, SDS and sulfuric acid was  $2 \times 10^{-3}$ ,  $2 \times 10^{-3}$  and 0.2 mol L<sup>-1</sup>, respectively.

### 3.4 Analytical features of FIA method

Analytical features of the FIA system at the optimal condition as described in 3.3 were evaluated. In the range of 1-150 mg L<sup>-1</sup>, the calibration graph was linear and described by Eq. (3.1):

$$y = 0.3035x - 0.3834, \quad (3.1)$$

where  $R^2 = 0.9998$ ,  $x$  refers to [PR] (mg L<sup>-1</sup>) and  $y$  is the peak height (mV). The limit of detection (3 S/N) was 0.75 mg L<sup>-1</sup> and %RSD of 10-replicate injection and intraday precision was 1.7. and 2.9. The recovery by standard addition method was studied by mixing the sample solution with 5.0, 10.0, 15.0, 20.0 and 25.0 mg L<sup>-1</sup> of PR. The standards were found at the concentrations of 5.4, 10.4, 15.4, 20.0 and 25.1 mg L<sup>-1</sup>, respectively, and percentage recoveries were 108, 104, 103, 100 and 100. The sample throughput of this proposed method was 50 h<sup>-1</sup>.

Table 1 compares some analytical features of existing colorimetric methods and the proposed method. The proposed method provided a wider linear range with an acceptable detection limit than other colorimetric methods. It is suitable for use in pharmaceutical determination, especially in routine analysis, due to its lower cost and lower reagent consumption. Moreover, with simple reagent and method, it can be easily setup in most laboratories.

### 3.5 FIA Application for real sample analysis

This proposed method was applied to determine PR in procaine hydrochloride tablets (100 mg per tablet, Romania and USA Anti-aging products) and injection (2 % w/v of PR) and compared to USP 2004

method that used chloroform extraction and measure the absorption at 280 nm. Table 2 summarizes our findings. By using T-test, we observed no significant differences between the results of these two methods at 95% confidence limit.

**Table 1.** Comparison of some analytical features of this proposed method to other colorimetric methods in determination of PR.

Year	Colorimetric reagent	$\lambda_{\max}/\text{nm}$	Linearity /mg L <sup>-1</sup>	LOD / mg L <sup>-1</sup>	Reference
2022	Ce(SO <sub>4</sub> ) <sub>2</sub> . 4H <sub>2</sub> O in H <sub>2</sub> SO <sub>4</sub> with SDS sensitizing	513	1-150	0.75	This proposed method
2015	NaNO <sub>2</sub> /HCl, Phenol and NH <sub>4</sub> OH (10°C)	450	2-22	1.29	A.U. Wasan [18]
2013	Fe(NO <sub>3</sub> ), Phenothiazine	610	2-80	-	M.Q. Al-Abachi [8]
2003	1,2-napthoquinone-4-sulfonic acid sensitized by SDS	484	0.30-100	0.28	L.X. Xu et al. [11]
2003	p-benzoquinone in ethanol	525	5-90	-	A.S. Amin and A.M. El-Didamony [10]
2000	p-dimethylamino-benzaldehyde in glacial acetic acid	455	0.2-15	0.1	L.D. Liu et al. [9]
1992	4-dimethylamino-cinnamaldehyde (40°C)	547	0.5-20	0.1	M. Carmona et al. [12] (stop flow)
1989	Iron(III)	540	80-1120	40	J.Novakovic [14]

**Table 2.** The determination of PR in procaine hydrochloride injections and tablets by the proposed method compared to USP 2004 [17].

Samples	Labelled*	PR in dosage unit* (± SD)	
		FIA	USP
Injection A	1	1.02 ± 0.02	0.98 ± 0.03
Injection B	1	1.06 ± 0.02	0.95 ± 0.03
Injection C	2	2.08 ± 0.04	2.02 ± 0.04
Injection D	2	1.87 ± 0.04	1.98 ± 0.04
Injection E	2	2.03 ± 0.06	1.85 ± 0.06
Tablet A	100	94.1 ± 2.0	90.7 ± 3.1
Tablet B	100	91.0 ± 2.1	92.9 ± 2.9
Tablet C	100	91.0 ± 2.9	99.6 ± 2.5
Tablet D	100	92.5 ± 2.1	96.2 ± 3.8
Tablet E	100	91.1 ± 1.5	97.3 ± 2.1

\*Dosage units of Injection and Tablets are labelled in the unit of % w/v and mg/tablets, respectively

### 3.6 Computational investigation of the Ce(IV)/PR complex

Table 3 summarizes all possible binding configurations of Ce(IV) complexes with all organic ligands with their energies

being relative to that of system 1.6. For Ce(IV)/procaine, six binding configurations were located. The most stable configuration was 1.2 which has Ce(IV) bound to the carbonyl oxygen. Its B3LYP/SDD energy was 3.69 kcal mol<sup>-1</sup> less than that of 1.6. System 1.6 which Ce(IV) binds to the tertiary amino nitrogen is of lower energy than system 1.1 which Ce(IV) binds to the primary amino nitrogen with the binding energy of 4-5 kcal mol<sup>-1</sup>. This is expected since the tertiary amino nitrogen atom is a better electron donating atom than the primary one. The configuration which Ce(IV) binds to the ester oxygen was higher in energy than the other monodentate configurations. This is not surprising because the ester oxygen is a less common donor atom [39].

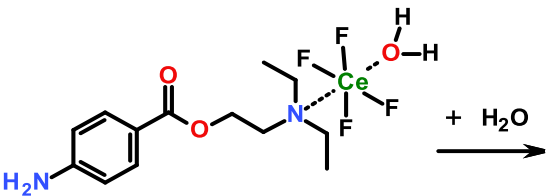
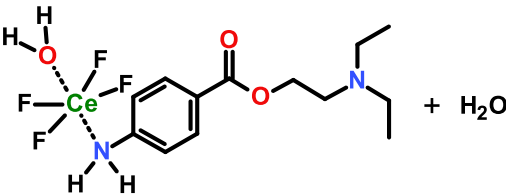
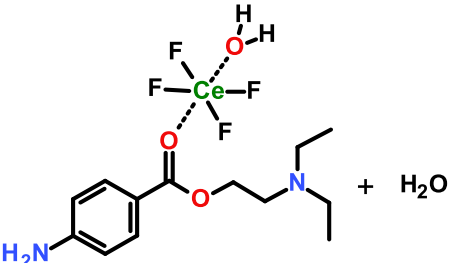
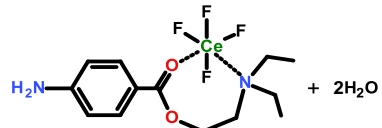
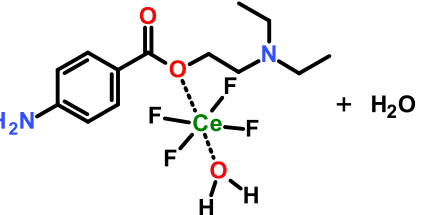
Both bidentate configurations with Ce(IV) forming five- and seven-membered rings with procaine (configurations 1.5 and

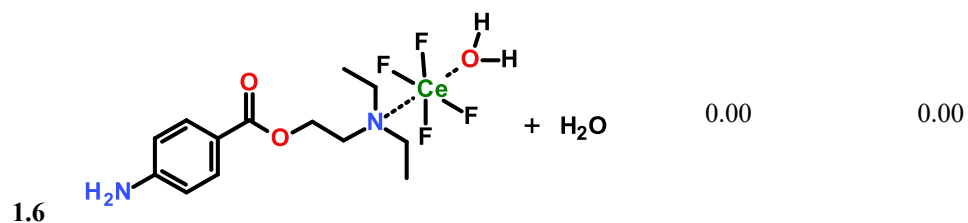
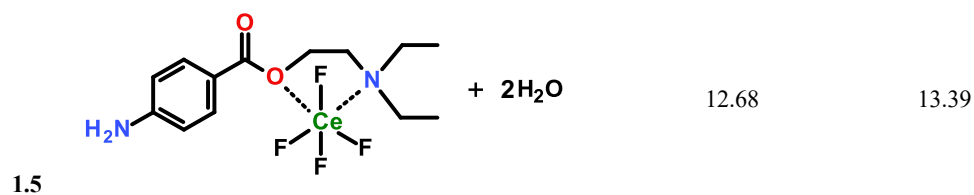


1.3) were both higher in energy than the monodentate configurations. However, the

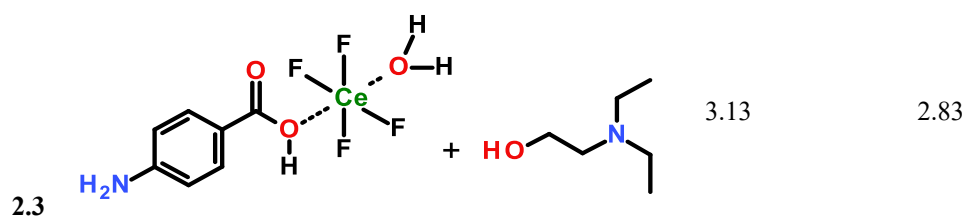
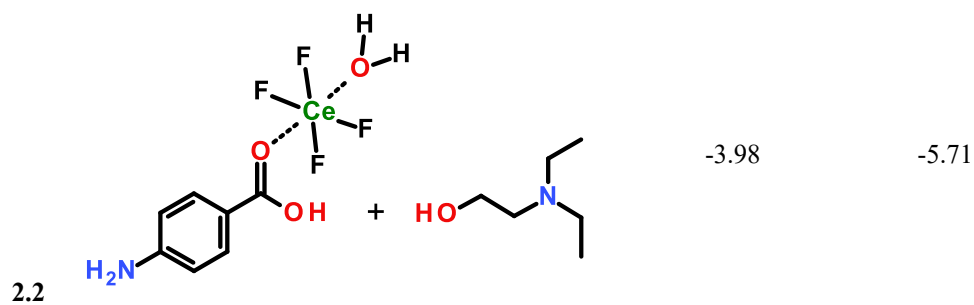
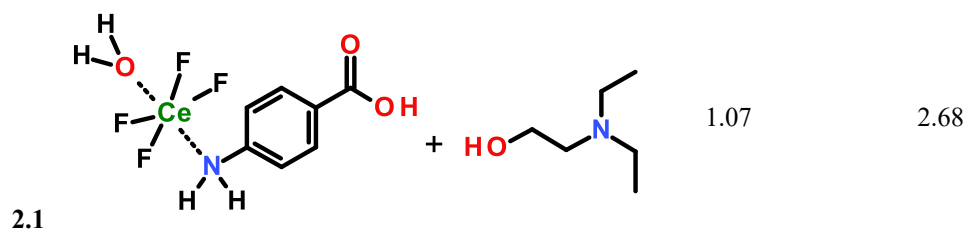
entropic contributions of bidentate configurations should be more favorable than that of monodentate configurations.

**Table 3.** The relative energy of Ce(IV) forming complex with 1) procaine 2) PABA and 3) DEAE. System 1.6 was arbitrarily chosen as the reference system.

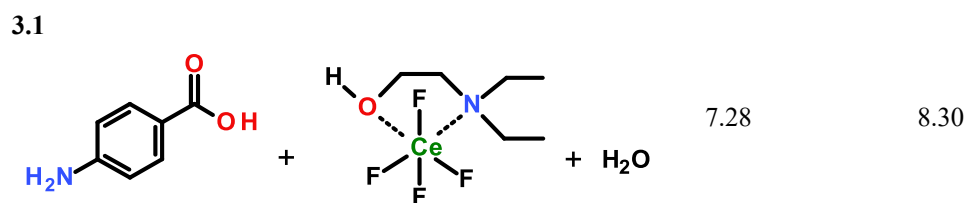
System/Method		$\Delta E$ / (kcal/mol)	
		BP86/SDD/AUTO	B3LYP/SDD
			
Ce(IV)/procaine			
1.1		4.43	5.32
1.2		-3.71	-3.69
1.3		9.09	8.72
1.4		6.01	6.98



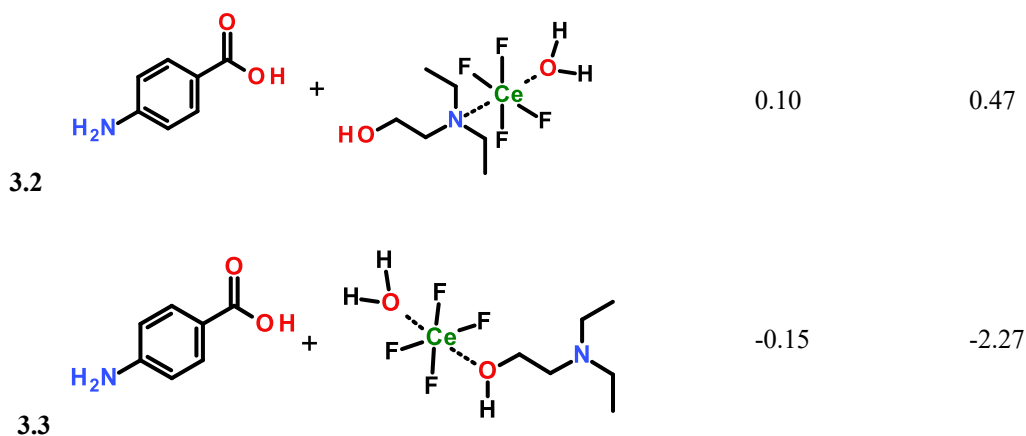
Ce(IV)/PABA



Ce(IV)/DEAE



## Ce(IV)/DEAE

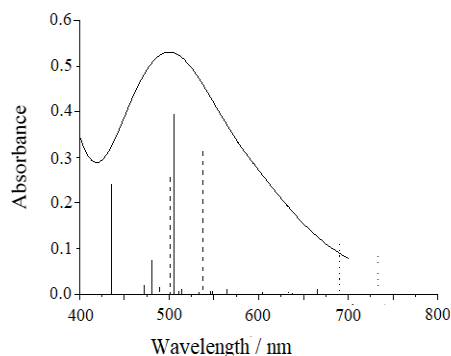


The Ce(IV)/PABA complexes had three possible binding configurations (see Table 3). Configuration 2.2, in which Ce(IV) binds to the carbonyl oxygen, was the most stable configuration. This is the same configuration as observed in Ce(IV)/procaine. Its B3LYP/SDD energy was  $5.71 \text{ kcal mol}^{-1}$  less than that of 1.6. Considering all configurations in which Ce(IV) binds with the same donor atom, the energy of the Ce(IV)/PABA complex is less than that of the Ce(IV)/procaine complex. This agrees with the observation that the hydrolysis of the ester bond releases energy [40].

For the Ce(IV)/DEAE complexes, three binding configurations were located. We see yet again that the bidentate system 3.1 is greater in energy than the monodentate configuration. The lowest energy configuration was 3.3, in which Ce(IV) binds with the hydroxyl oxygen. However, this configuration was not preferred over the most stable configurations of the Ce(IV)/procaine and Ce(IV)/PABA complexes, in which Ce(IV) binds to the carbonyl oxygen. This was confirmed by the TDDFT results which will

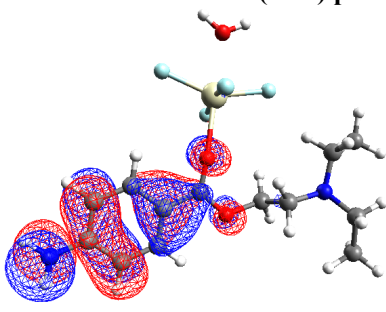
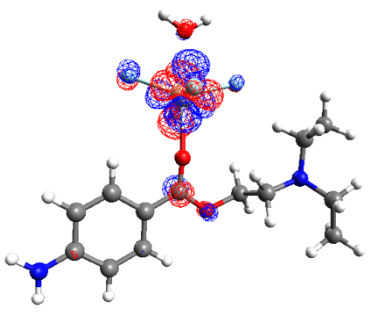
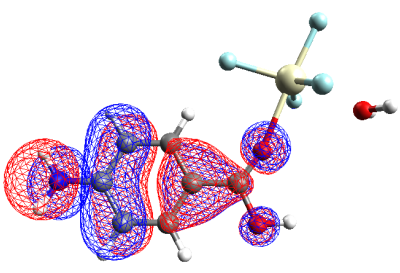
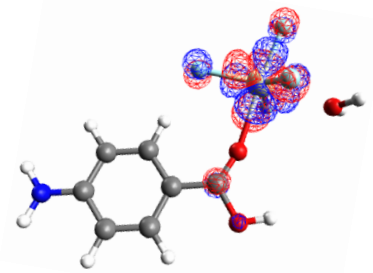
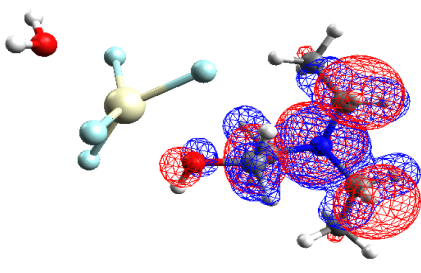
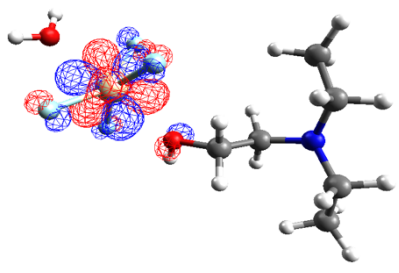
be discussed next. Energetically, the Ce(IV)/PABA complex is the most stable system among the three complexes.

The electronic excitations of these complexes were calculated by using the TD-PBE0/SDD method (see Fig. 7 and Table 4).



**Fig. 7.** The TD-PBE0/SDD//B3LYP/SDD electronic excitation of Ce(IV)/procaine (solid), Ce(IV)/PABA (dash) and Ce(IV)/DEAE (dot) complexes. Overlaid curve is the experimental absorption spectra of Ce(IV):procaine mixture at 0.0007 and 0.0167 M. The oscillator strength is arbitrarily scaled.

**Table 4.** The first major electronic transition in the visible region of the Ce(IV)/procaine, Ce(IV)/PABA and Ce(IV)/DEAE complexes. The most stable binding configurations are used for all complexes.

$\lambda/\text{nm}$ ( <i>f</i> )	Initial MO	Final MO
<b>CeF<sub>4</sub>(H<sub>2</sub>O)/procaine</b>		
505(0.0194)	 HOMO-1	 LUMO+1
<b>CeF<sub>4</sub>(H<sub>2</sub>O)/PABA</b>		
537(0.0154)	 HOMO	 LUMO+2
<b>CeF<sub>4</sub>(H<sub>2</sub>O)/DEAE</b>		
734(0.0041)	 HOMO	 LUMO+2

A preliminary TDDFT calculation on free procaine yielded a strong excitation at 286 nm which is in excellent agreement with the experimental absorption at 290 nm. We conducted a TDDFT calculation on  $\text{Ce(IV)F}_4(\text{H}_2\text{O})_2$  and found no excitation in the visible region.

Fig. 7 displays the absorption spectrum of the  $\text{Ce(IV)}$ :procaine mixture in the visible region alongside electronic excitations from the most stable form of each  $\text{Ce(IV)}$  complex. The observed  $\text{Ce(IV)}$ :procaine solution was brownish red. The absorption maximum wavelength was about 500 nm. The  $\text{Ce(IV)/DEAE}$  complex had very weak calculated peaks close to 700 nm. It is apparent that the  $\text{Ce(IV)/DEAE}$  complex could not account for the experimental absorption. The TDDFT result clearly eliminated the possibility of a  $\text{Ce(IV)/DEAE}$  complex in the solution.

On the other hand, the electronic excitations of  $\text{Ce(IV)/procaine}$  and  $\text{Ce(IV)/PABA}$  agreed well with the observed spectrum. We should not overstate such agreement because of the simple model used in our treatment, although we carefully chose the  $\{\text{Ce(IV)F}_4\}$  metal fragment based on the proximity of the fluoride anion to the  $\text{H}_2\text{O}$  ligand in the spectrochemical series [20-22].  $\text{Ce(IV)/procaine}$  had the first strong peak at 505 nm, whereas in the case of  $\text{Ce(IV)/PABA}$  it was at 537 nm. The excitation of both complexes is rather similar as it involves almost the same chromophore. The oscillator strength of the corresponding transition around 500 nm of  $\text{Ce(IV)/procaine}$  was greater than that of the  $\text{Ce(IV)/PABA}$  complex. Considering the character of involved orbitals, the first major transition in all possible complexes can be characterized as the ligand-to-metal transition. The  $\text{Ce(IV)/PABA}$  and  $\text{Ce(IV)/procaine}$  complexes have the  $\pi$  electron transferred to the metal unoccupied orbital while the  $\text{Ce(IV)/DEAE}$  complex has

the lone pair transferred to the metal unoccupied orbital.

From the spectrum alone, it cannot be concluded that the brownish-red color observed in experiment results from the complex of cerium(IV) with either procaine or PABA. Taking the relative energy into account, it is more likely that the dominant complex is  $\text{Ce(IV)/PABA}$  with cerium binding to the carbonyl oxygen. Initially the  $\text{Ce(IV)/procaine}$  complex might be formed but the bonding of  $\text{Ce(IV)}$  should facilitate the conversion of procaine to PABA as this increases the electropositive nature of procaine carbonyl carbon; hence, also giving  $\text{Ce(IV)/PABA}$  in the solution mixture. This is in accordance with what Kassai et al. [41] and Takarada et al.[42] observed in phosphate ester and peptide systems, respectively.

#### 4. Conclusion

Our proposed method for the determination of procaine hydrochloride by FIA with colorimetric detection based on the reaction of PR and  $\text{Ce(IV)}$  with SDS sensitizer was successful. The computational investigation suggests that the  $\text{Ce(IV)/PABA}$  is the complex attributed to the red color of the solution. The good recovery, linearity, precision and detection limit was obtained. It was successfully applied to determine PR in the preparations with the same precision obtained by the standard method (USP 2004). This FIA method is more eco-friendly. Due to its simplicity, it can be easily set up and readily made available for most laboratories.

#### Acknowledgements

The authors would like to acknowledge Thammasat University Research Unit in Carbon Materials and Green Chemistry Innovations for funding in this research. We thank NARIT for providing computing time on Chalawan HPC cluster.

## References

- [1] Reynolds JEF, editor. Martindale: The extra pharmacopoeia. 30th ed. London: Pharmaceutical Press; 1993.
- [2] Dhananjeyan M, Trendel J, Bykowski-Jurkiewicz C, Sarver J, Ando H, Erhardt P. Rapid and sensitive HPLC assay for simultaneous determination of procaine and p-aminobenzoic acid from human and rat liver tissue extracts. *J Chromatogr B* 2008;867:247-52.
- [3] Storms ML, Stewart JT. Stability-indicating HPLC assays for the determination of prilocaine and procaine drug combinations. *J Pharm Biomed* 2002;30(1):49-58.
- [4] Michalska K, Pajchel G, Tyski S. Capillary electrophoresis method for simultaneous determination of penicillin G, procaine and dihydrostreptomycin in veterinary drugs. *J Chromatogr B* 2004;800(1-2):203-9.
- [5] Wu K, Wang H, Chen F, Hu S. Electrochemistry and voltammetry of procaine using a carbon nanotube film coated electrode. *Bioelectrochemistry* 2006;68:144-9.
- [6] Khalaf M. Colorimetric determination of procaine hydrochloride in pharmaceutical preparations using diazotization coupling reactions. *Int J PharmTech Res* 2015;8(5):1042-52.
- [7] Marin N, Batrinescu G, Nita-Lazar M, Pascu L, Lehr C. Simultaneous determination of procaine hydrochloride, procainamide hydrochloride and lidocaine by molecular absorption spectrometry. *Proceeding of the International Symposium The Environmental and The Industry*. 2019 Sep 26-27; Bucharest, Romania; 2019:318-24.
- [8] Al-Abachi M, Al-Ward H, Al-Samarrai E. Spectrophotometric Determination of procaine hydrochloride in pharmaceutical preparation via oxidative coupling reaction. *Tikrit J Pharm Sci* 2013; 9(2):213-22.
- [9] Liu LD, Liu Y, Wang HY, Sun Y, Ma L, Tang B. Use of p-dimethylaminobenzaldehyde as a colored reagent for determination of procaine hydrochloride by spectrophotometry. *Talanta*. 2000; 52(6):991-9.
- [10] Amin AS, El-Didamony AM. Colorimetric determination of benzocaine, lignocaine and procaine hydrochlorides in pure form and in pharmaceutical formulations using p-benzoquinone. *Anal Sci* 2003;19(10): 1457-9.
- [11] Xu LX, Shen YX, Wang HY, Jiang JG, Xiao Y. Spectrophotometric determination of procaine hydrochloride in pharmaceutical products using 1,2-naphthoquinone-4-sulfonic acid as the chromogenic reagent. *Spectrochim Acta A Mol Biomol* 2003;59(13):3103-10.
- [12] Carmona M, Silva M, Perez-Bendito D. A selective and sensitive kinetic method for the determination of procaine and benzocaine in pharmaceuticals. *J Pharm Biomed* 1992;10(2-3):145-52.
- [13] Bartos J, Pesez M. Spectrophotometric and fluorimetric determination of amines. *Pure Appl Chem* 1984;56(4):467-77.
- [14] Novaković J. Spectrophotometric determination of procaine hydrochloride by means of iron (3+)-4-aminobenzohydroxamic acid complex. *Boll Chim Farm* 1989;128(12):370-2.
- [15] Li N, Chi Y, Wang J, Duan J, Chen G. Determination of procaine hydrochloride using flow injection inhibitory chemiluminescence. *Luminescence*. 2003;18(3):125-30.
- [16] Sun Y, Ma L, Wang H-y, Tang B. Determination of procaine hydrochloride by fluorimetry]. *Guang Pu Xue Yu Guang Pu Fen Xi* 2002;22(4):637-40.



- [17] United States Pharmacopeial Convention: National Formulary; 2004.
- [18] Al-Uzri W. Spectrophotometric Determination of Procaine Hydrochloride in Pharmaceutical Preparations via Diazotization-Coupling Reaction with Phenol. *Asian J Chem* 2015;27:4449-53.
- [19] Parpot P, Teixeira C, Almeida AM, Ribeiro C, Neves IC, Fonseca AM. Redox properties of (1-(2-pyridylazo)-2-naphthol)copper(II) encapsulated in Y Zeolite. *Microporous Mesoporous Mater* 2009;117(1-2):297-303.
- [20] Bersuker IB. *Electronic Structure and Properties of Transition Metal Compounds: Introduction to the Theory* New York: John Wiley & Sons; 2009.
- [21] Jorgensen CK. *Oxidation Numbers and Oxidation States*. Berlin: Springer-Verlag; 1969.
- [22] Jorgensen CK. *Modern aspects of ligand field theory*. Amsterdam: North-Holland Pub. Co; 1971.
- [23] Braier NC, Jishi RA. Density functional studies of  $\text{Cu}^{2+}$  and  $\text{Ni}^{2+}$  binding to chitosan. *J Mol Struct* 2000;499(1-3):51-5.
- [24] Schuchardt KL, Didier BT, Elsethagen T, Sun L, Gurumoorthi V, Chase J, et al. Basis set exchange: A community database for computational sciences. *J Chem Inf Model* 2007;47(3):1045-52.
- [25] Dolg M, Stoll H, Preuss H. A combination of quasirelativistic pseudopotential and ligand field calculations for lanthanoid compounds. *Theor Chim Acta* 1993;85(6):441-50.
- [26] Cossi M, Rega N, Scalmani G, Barone V. Energies, structures, and electronic properties of molecules in solution with the C-PCM solvation model. *J Comput Chem* 2003;24(6):669-81.
- [27] Li YL, Han L, Mei Y, Zhang JZH. Time-dependent density functional theory study of absorption spectra of metallocenes. *Chem Phys Lett* 2009;482(4-6):217-22.
- [28] Burke K, Werschnik J, Gross EKV. Time-dependent density functional theory: Past, present, and future. *J Chem Phys* 2005;123(6):1-9.
- [29] Jian W, Fu-Quan B, Bao-Hui X, Lei S, Hong-Xing Z. Theoretical Understanding of Ruthenium(II) Based Fluoride Sensor Derived from 4,5-Bis(benzimidazol-2-yl)imidazole (H3ImBzim) and Bipyridine: Electronic Structure and Binding Nature. *J Phys Chem A* 2011;115(10):1985-91.
- [30.] Escudero D, Trupp S, Bussemer B, Mohr GJ, González L. Spectroscopic properties of azobenzene-based pH indicator dyes: A quantum chemical and experimental study. *J Chem Theory Comput* 2011; 7(4):1062-72.
- [31] Frisch MJ, Trucks GW, Schlegel HB, Scuseria GE, Robb MA, Cheeseman JR, et al. *Gaussian 09*. Wallingford: Gaussian, Inc; 2009.
- [32] Hanwell MD, Curtis DE, Lonie DC, Vandermeersch T, Zurek E, Hutchison GR. Avogadro: An advanced semantic chemical editor, visualization, and analysis platform. *J Cheminf* 2012;4:1-17.
- [33] Rudbeck M. Basis Set Dependence of Phosphate Frequencies in Density Functional Theory Calculations. *Int J Quant Chem* 2012;112: 2435-9.
- [34] Wang AJ, Fan J, Feng SL, Cui FL, Spectral study and determination of metoclopramide and procaine hydrochloride by sequential injection analysis. *Guang Pu Xue Yu Guang Pu Fen Xi* 2005;25(3):432-5.
- [35] Kitamura Y, Sumaoka J, Komiyama M. Hydrolysis of DNA by cerium(IV)/EDTA

- complex. Tetrahedron 2003;59(52):10403-8.
- [36] Yoshikuni T. Cerium complexes with phthaloylbis(pyrazolone) ligands as an efficient catalysts for cresols dioxygenation. J Mol Catal A Chem 1999;148(1-2):285-8.
- [37] Ahmed IS, Amin AS, Issa YM. The surfactant sensitized analytical reaction of cerium(IV) with some triphenylformazan derivatives. Spectrochim Acta A Mol Biomol 2006;64(1):246-50.
- [38] Gürcan R, Ulusoy HI, Akçay M. Surfactant enhanced-spectrophotometric determination of uranium (VI) at trace levels by using eriochrome black T as a chelating agent. Eclética Química 2011;36(3):37-46.
- [39] Molčanov K, Kojić-Prodić B, Raos N. Analysis of the less common hydrogen bonds involving ester oxygen  $sp^3$  atoms as acceptors in the crystal structures of small organic molecules. Acta Crystallogr B Struct Sci Cryst Eng Mater 2004;60(4):424-32.
- [40] Testa B, Mayer JM, editors. Hydrolysis in drug and prodrug metabolism, chemistry, biochemistry and enzymology. Zürich: Verlag Helvetica Chimica Acta; 2003.
- [41] Kassai M, Teopipithaporn R, Grant KB. Hydrolysis of phosphatidylcholine by cerium(IV) releases significant amounts of choline and inorganic phosphate at lysosomal pH. J Inorg Biochem 2011; 105(2):215-23.
- [42] Takarada T, Yashiro M, Komiyama M. Catalytic hydrolysis of peptides by cerium(IV). Chemistry 2000;6(21):3906-13.